

Finite temperature off-diagonal long-range order for interacting bosons

A. Colcelli¹, N. Defenu^{2,3}, G. Mussardo¹ and A. Trombettoni^{4,5,1}

¹SISSA and INFN, Sezione di Trieste, Via Bonomea 265, I-34136 Trieste, Italy

²Institute for Theoretical Physics, ETH Zürich, Wolfgang-Pauli-Str. 27, 8093 Zürich, Switzerland

³Institute for Theoretical Physics, Heidelberg University, D-69120 Heidelberg, Germany

⁴Department of Physics, University of Trieste, Strada Costiera 11, I-34151 Trieste, Italy

⁵CNR-IOM DEMOCRITOS Simulation Center, Via Bonomea 265, I-34136 Trieste, Italy



(Received 14 July 2020; revised 1 September 2020; accepted 1 September 2020; published 17 November 2020)

Characterizing the scaling with the total particle number (N) of the largest eigenvalue of the one-body density matrix (λ_0) provides information on the occurrence of the off-diagonal long-range order (ODLRO) according to the Penrose-Onsager criterion. Setting $\lambda_0 \sim N^{C_0}$, then $C_0 = 1$ corresponds in ODLRO. The intermediate case, $0 < C_0 < 1$, corresponds in translational invariant systems to the power-law decaying of (nonconnected) correlation functions and it can be seen as identifying quasi-long-range order. The goal of the present paper is to characterize the ODLRO properties encoded in C_0 (and in the corresponding quantities $C_{k \neq 0}$ for excited natural orbitals) exhibited by homogeneous interacting bosonic systems at finite temperature for different dimensions in presence of short-range repulsive potentials. We show that $C_{k \neq 0} = 0$ in the thermodynamic limit. In one dimension it is $C_0 = 0$ for nonvanishing temperature, while in three dimensions it is $C_0 = 1$ ($C_0 = 0$) for temperatures smaller (larger) than the Bose-Einstein critical temperature. We then focus our attention to $D = 2$, studying the XY and the Villain models, and the weakly interacting Bose gas. The universal value of C_0 near the Berezinskii-Kosterlitz-Thouless temperature T_{BKT} is $7/8$. The dependence of C_0 on temperatures between $T = 0$ (at which $C_0 = 1$) and T_{BKT} is studied in the different models. An estimate for the (nonperturbative) parameter ξ entering the equation of state of the two-dimensional Bose gases is obtained using low-temperature expansions and compared with the Monte Carlo result. We finally discuss a “double jump” behavior for C_0 , and correspondingly of the anomalous dimension η , right below T_{BKT} in the limit of vanishing interactions.

DOI: [10.1103/PhysRevB.102.184510](https://doi.org/10.1103/PhysRevB.102.184510)

I. INTRODUCTION

Off-diagonal long-range order (ODLRO) in the one-body density matrix (1BDM) of Bose particles signals the appearance of Bose-Einstein condensation (BEC) in quantum systems. This relation is established by the Penrose-Onsager criterion [1] which applies in all dimensions D and at any temperature T , irrespectively of the presence of confining potentials. For its versatility, it constitutes a simple way to determine whether a quantum Bose gas exhibits condensation and coherence effects [2,3].

For $D \leq 2$ the Mermin-Wagner theorem [4,5] ensures that, for translational invariant systems with continuous symmetry such as interacting bosons or $O(N)$ spin models with $N \geq 2$, no long-range order can be found at finite temperature. Indeed, the theorem forbids the occurrence of spontaneous symmetry breaking for $T > 0$ in low-dimensional systems, where the symmetry of the Hamiltonian is restored by the proliferation of long-wavelength fluctuations. For a Bose gas the Goldstone modes are represented by the phonons, which in $D = 2$ destroy long-range order, leaving low-temperature superfluidity intact. In such case, due to the persistence of $U(1)$ symmetry, the equilibrium finite-temperature average of the bosonic field operator $\hat{\Psi}$ vanishes, due to the lack of phase coherence [3]. This can be seen occurring when the scaling dimension of

the bosonic field $\hat{\Psi}$ becomes zero [6]. It is worth noting that a similar effect takes place in a wide range of systems with long-range interactions, even if the Mermin-Wagner theorem does not strictly apply [7,8]. A space version of the Mermin-Wagner theorem, where a relation between the size of a condensate and the coherence properties of the gas is established, is discussed in Ref. [9].

A compact way to define ODLRO is to introduce the 1BDM [10]

$$\rho(\vec{x}, \vec{y}) = \langle \hat{\Psi}^\dagger(\vec{x}) \hat{\Psi}(\vec{y}) \rangle, \quad (1)$$

where the field operator $\hat{\Psi}(\vec{x})$ destroys a particle at the point identified by the D -dimensional vector \vec{x} . The 1BDM, as an Hermitian matrix, satisfies the eigenvalue equation

$$\int \rho(\vec{x}, \vec{y}) \phi_i(\vec{y}) d\vec{y} = \lambda_i \phi_i(\vec{x}), \quad (2)$$

with the eigenvalues λ_i being real. They denote the occupation number of the i th natural orbital eigenfunction ϕ_i , with $\sum_i \lambda_i = N$, where N is the total number of particles. The occurrence of ODLRO (and therefore of BEC) is characterized by a linear scaling of the largest eigenvalue λ_0 with respect to the total number of particles N in the system [1,11]: $\lambda_0 \sim N$.

For a translational invariant system, the indices i in Eq. (2) are wave vectors, which are conventionally denoted by the vector \vec{k} . Introducing the scaling formula

$$\lambda_0 \sim N^{C_0(T)}, \quad (3)$$

the Mermin-Wagner theorem implies that $C_0(T) < 1$ for $T > 0$ and $D \leq 2$, so there is no ODLRO at finite temperature. At variance, there is ODLRO/BEC whenever $C_0 = 1$. One can show as well that $C_0(T = 0) = 1$ for $D = 2$ and $C_0(T = 0) < 1$ in $D = 1$ (for the interacting case) (see Ref. [12]). For a translational invariant system, the absence of ODLRO, or equivalently of BEC, in $D = 2$ at finite temperature amounts to the following behavior of the 1BDM at large distances:

$$\langle \hat{\Psi}^\dagger(\vec{x})\hat{\Psi}(\vec{y}) \rangle \xrightarrow{|\vec{x}-\vec{y}| \rightarrow \infty} \langle \hat{\Psi}(\vec{x}) \rangle^* \langle \hat{\Psi}(\vec{y}) \rangle = 0. \quad (4)$$

The existence and regimes for BEC, i.e., whether $C_0 = 1$ or not, in various physical systems has been the subject of a remarkable amount of work. It would be therefore desirable to complete such analysis with a systematic study of when C_0 is smaller than 1: In this case there is no ODLRO/BEC but nevertheless the condition $0 < C_0 < 1$ implies that, in translational invariant systems, the correlation function $\langle \hat{\Psi}^\dagger(\vec{x})\hat{\Psi}(\vec{y}) \rangle$ has a power-law decay. One may refer to this situation as *quasi-long-range order*.

The relation between the scaling behavior of density matrices of any order (including the one-body density matrix considered in the present work) and the types of order characterizing the physical system were analyzed in Ref. [13], where the so-called order indices were introduced and studied both for certain fermionic and bosonic systems. Since the order index for the n th-order reduced density matrix is defined as $\alpha^{(n)} = \lim_{N \rightarrow \infty} \ln \lambda_0^{(n)} / \ln N$, where $\lambda_0^{(n)}$ is the largest eigenvalue of the n th-order density matrix, then we can identify the order index $\alpha^{(1)}$ of the 1BDM as the exponent $C_0(T)$ defined in Eq. (3) from the scaling of $\lambda_0 \equiv \lambda_0^{(1)}$. The concept of order indices can be extended to arbitrary matrices (see Ref. [14] for a discussion), while the relation between order indices and entanglement production is discussed in Ref. [15].

Here, we study ODLRO properties in terms of the scaling with the particles number N of the eigenvalues λ_k of the 1BDM, both of the largest eigenvalue λ_0 and of the others $\lambda_{k \neq 0}$. Let us stress that, for a system of interacting bosons, the index C_0 may also depend on the interaction strength and, moreover, one may expect that increasing the repulsion among the bosons, C_0 gets dampened with respect to the weak interacting case, as seen explicitly in the one-dimensional (1D) case at zero temperature [16].

In the present work, we are going to characterize ODLRO, and possible deviations from it, in translational invariant bosonic systems interacting via short-range repulsive potentials in one, two and three dimensions at finite temperature. With “possible deviations” we also mean a study of the behavior of the index $C_k(T)$, defined as

$$\lambda_k \sim N^{C_k(T)}, \quad (5)$$

where $k \neq 0$. The study of $C_{k \neq 0}(T)$ gives an insight about the possible *quasi-fragmentation* of the system, i.e., how the

particles occupy the other, $k \neq 0$, states. Notice that in literature usually one refers to fragmentation when more than one eigenvalue of the 1BDM scales with N . So, one can refer to the case in which at least two C_k are larger than zero (and at least one is smaller than 1) as a quasi-fragmentation.

We observe that there is a mesoscopic condensate (i.e., quasi-long-range order), with a finite value for the condensate fraction $\frac{\lambda_0}{N}$ for finite values of N , for $0 < C_0(T) < 1$. In this case the condensate fraction of course vanishes for $N \rightarrow \infty$ but, even though the system is not a true BEC, one would observe nevertheless a clear peak in the momentum distribution in an experiment with ultracold gases: The reason is that the number of particles which are typically used in these apparatus are of order $N \sim 10^3 - 10^5$, and therefore the condensate fraction $\frac{\lambda_0}{N} \sim \frac{N^{C_0(T)}}{N}$ could be very close to the unity for $C_0(T)$ close to 1. For $C_0(T) = 0$ there will be no order at all, and the system qualitatively behaves, from the point of view of the eigenvalues of the 1BDM, like a Fermi gas.

The plan of the paper is the following. In Sec. II we discuss the relation between the 1BDM and the momentum distribution, setting the notation for the following sections. The cases $D = 3$ and $D = 1$ are discussed respectively in Secs. III and IV: these two cases provide the reference frame and the warming up for the discussion of the finite temperature ODLRO properties of two-dimensional Bose gases in Sec. V. In Sec. V we also present a study of the ODLRO in the XY and the Villain models. Our conclusions are presented in Sec. VI.

II. MOMENTUM DISTRIBUTION OF HOMOGENEOUS SYSTEMS

The advantage of studying how the largest eigenvalue scales with the number of particles, instead of the large distance behavior of the 1BDM, becomes evident once we define another important quantity: the momentum distribution. To introduce this quantity, let us initially consider the Fourier transform $\hat{\Psi}(\vec{k})$ of the field operator $\hat{\Psi}(\vec{x})$:

$$\hat{\Psi}(\vec{k}) = \frac{1}{(2\pi)^{D/2}} \int d\vec{x} e^{i\vec{k}\cdot\vec{x}} \hat{\Psi}(\vec{x})$$

and the momentum distribution $n(k)$ given by

$$\begin{aligned} n(\vec{k}) &= \langle \hat{\Psi}^\dagger(\vec{k})\hat{\Psi}(\vec{k}) \rangle \\ &= \frac{1}{(2\pi)^D} \int d\vec{x} \int d\vec{y} e^{i\vec{k}\cdot(\vec{x}-\vec{y})} \langle \hat{\Psi}^\dagger(\vec{x})\hat{\Psi}(\vec{y}) \rangle. \end{aligned} \quad (6)$$

For a homogeneous system, $\rho(x, y) = \langle \hat{\Psi}^\dagger(\vec{x})\hat{\Psi}(\vec{y}) \rangle$ depends only on the distance among two points, therefore writing the relative distance vector as $\vec{r} = \vec{x} - \vec{y}$, we can rewrite $\rho(\vec{x}, \vec{y}) = \rho(\vec{r})$ and assume $\rho(\vec{r}) = \rho(|\vec{r}|) \equiv \rho(r)$. Passing to center of mass and relative coordinates, since $\int d\vec{R} = L^D$ where L denotes the size of the system (e.g., L is the circumference of a ring in one-dimensional geometry), Eq. (6) can be rewritten as

$$n(\vec{k}) = \left(\frac{L}{2\pi} \right)^D \int e^{i\vec{k}\cdot\vec{r}} \rho(r) d\vec{r}. \quad (7)$$

The integral in the right-hand side depends of course on the dimension D . Notice that the momentum distribution peak is

simply given by the integral of the 1BDM

$$n(\vec{k} = 0) = \left(\frac{L}{2\pi}\right)^D \int \rho(r) d\vec{r}, \quad (8)$$

and, as expected, the large distance asymptotic of the 1BDM determines the small momenta behavior of the momentum distribution.

For a homogeneous, isotropic system the quantum number labeling the occupation of natural orbitals clearly depends on the wave vector modulus $|\vec{k}| \equiv k$. In particular, the Galilean invariance tells us that the effective single-particle states $\phi_k(\vec{x})$ may be written as plane waves, i.e., $\phi_k(\vec{x}) = \frac{1}{L^{D/2}} e^{i\vec{k}\cdot\vec{x}}$, therefore from Eqs. (2) and (7) we obtain that the dimensionless momentum distribution, $n(\vec{k})/L^D$, coincides with the eigenvalue equation of the one-body density matrix, apart from a $(1/2\pi)^D$ factor. Therefore, for a homogeneous system we have a one-to-one correspondence between the scaling of the eigenvalues of $\rho(r)$ and the scaling of the dimensionless momentum distribution:

$$\lambda_k \sim N^{C_k(T)} \sim \frac{n(k)}{L^D}. \quad (9)$$

The advantage of characterizing the different types of order in terms of the exponent $C_k(T)$ instead of the large distance behavior of the 1BDM is now clear and it stems from the fact that, in the experiments, it is easier to analyze the momentum distribution peak instead of looking at what happens to $\rho(\vec{x}, \vec{y})$ for very large (ideally infinite) distances $|\vec{x} - \vec{y}| \rightarrow \infty$, since one should discern with high precision if the 1BDM is zero or not at large distances.

Since a complete closed form for the density matrix is not in general available for all interaction strengths and temperatures, we cannot directly compute the eigenvalues of $\rho(\vec{x}, \vec{y})$ and then study their scaling with N . In order to obtain this information we will use the following procedure. From the large distance asymptotic behavior of the 1BDM, whose expression for different configurations of the system is usually available in the literature, we first make it a periodic function of period L by adding terms which have the same scaling behavior of the density matrix in the range $r \in [0, \frac{L}{2})$, and which represent the reflected parts in the range $(\frac{L}{2}, L]$. In this way we construct a fully symmetric and circulant matrix, whose eigenvalues are known to be real, as required, since they represent the occupation numbers of the system. Finally we perform the Fourier transform of this symmetrized density matrix and obtain in this way the behavior of the momentum distribution. Writing k as $k = \frac{2\pi}{L}l$ with $l \in \mathbb{N}$, the scaling of the largest eigenvalue of the 1BDM can be identified just imposing $l = 0$ and tracking its N dependence. In this way, we are able to explicitly compute the exponent $C_0(T)$ of the system. On the other hand, choosing $l \propto L$ the behavior of the Fourier transform in the limit $N \rightarrow \infty$ at fixed density $n = N/L^D$ yields the expression for the exponents $C_{k \neq 0}(T)$ via Eq. (9).

In the following, we aim to characterize the deviations from ODLRO at finite temperature for homogeneous interacting Bose gases in different dimensions. After discussing the explicit expression for C_0 , we will also discuss the finite

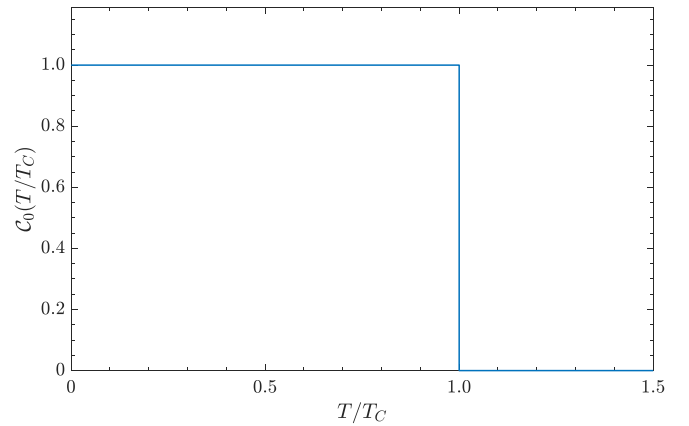


FIG. 1. Power $C_0(T/T_C)$ with which the momentum distribution peak of a homogeneous three-dimensional Bose gas scales with respect to the total number of particles N at different temperatures.

nonzero momenta landscape, ruling out the possibility of having quasi-fragmentation in bosonic interacting systems with repulsive interactions. Our findings provide a counterpart to the corresponding results for fragmentation in macroscopically occupied states with eigenvalues scaling with N [17].

III. THREE DIMENSIONS

Let us begin with the case of a three-dimensional homogeneous Bose gas. It is well known that, below the critical temperature T_C , a BEC takes place and the lowest allowed state for the gas is then macroscopically occupied [10]. This amounts to saying that the momentum distribution of the system is constituted by two parts: a nonsingular part, relative to the occupation of the single-particle states according to the Bose-Einstein distribution, and a singular part $\propto N_0 \delta(\vec{k})$ which refers to the macroscopic occupation $N_0 \propto N$ of the lowest energy state, also called the condensate state. Therefore, at $T < T_C$ ODLRO is found and the exponent will be $C_0 = 1$ in the condensed phase. For temperatures above the critical T_C there is no more condensation and the singular part of the momentum distribution, i.e., the Dirac delta peak, disappears together with the system ordering. From all of these facts one can conclude that

$$C_0(T) = \begin{cases} 1, & \text{for } T < T_C \\ 0, & \text{for } T > T_C, \end{cases} \quad (10)$$

as shown in Fig. 1.

In the weakly interacting Bose gas, one may use the Bogoliubov approximation [10] to obtain the scaling of the momentum distribution at $\vec{k} \neq 0$. Indeed, at this approximation level, the nonsingular part of the momentum distribution at $T < T_C$ reads

$$\frac{n(\vec{k})}{L^D} = \frac{1}{(2\pi)^3} \frac{1}{e^{\varepsilon(k)/k_B T} - 1}, \quad (11)$$

where $\varepsilon(k) = \sqrt{\frac{g\hbar}{m} \hbar^2 k^2 + \left(\frac{\hbar^2 k^2}{2m}\right)^2}$ is the Bogoliubov dispersion relation and $g = \frac{4\pi\hbar^2 a}{m}$ weights the interaction among particles in terms of the s -wave scattering length a . Therefore

for $\varepsilon(k)/k_B T \gg 1$ we obtain

$$\frac{n(\vec{k})}{L^D} \simeq \frac{1}{(2\pi)^3} e^{-\hbar^2 k^2 / 2mk_B T} \propto e^{-(l/L)^2} \propto N^0, \quad (12)$$

where in the second equality we used $k \propto l/L$, and in the last one we acknowledged that $l \propto L$ in order to have a finite momentum k in the thermodynamic limit. A similar procedure may be used to show the absence of quasi-fragmentation also for $T > T_C$, yielding

$$\mathcal{C}_{k \neq 0}(T) = 0 \quad (13)$$

at any temperature for the three-dimensional Bose gas. Notice that this result has been obtained using Bogoliubov theory and it may not be applicable to gases with nonweak interactions [18,19]. However, since the exponents \mathcal{C} are not expected to increase for larger interactions, one may reasonably conclude that this result is valid also for larger interactions.

IV. ONE DIMENSION

We now turn to the study of a one-dimensional homogeneous Bose gas [20,21], within the framework of the Lieb-Liniger model [22], where the interaction between particles is represented by a repulsive δ potential. The Lieb-Liniger Hamiltonian for N bosons of mass m then reads

$$H = -\frac{\hbar^2}{2m} \sum_{i=1}^N \frac{\partial^2}{\partial x_i^2} + 2c \sum_{i < j} \delta(x_i - x_j), \quad (14)$$

leading to the definition of the dimensionless coupling constant

$$\gamma = \frac{2mc}{\hbar^2 n}, \quad (15)$$

where $n = N/L$ is the density of the gas and L is the size of the system (with periodic boundary conditions this would be the circumference of the ring in which the system is enclosed). As is well known, the Lieb-Liniger model is exactly solvable by the Bethe-ansatz technique [22,23] which provides an exact expression for the many-body eigenfunctions [24,25]. Nevertheless, a closed expression for the 1BDM for every coupling γ and particle number N is not known. One should then rely both on approximations [26,27] and numerical approaches [16,28], which are suitable for working at large particle numbers.

At $T = 0$, techniques coming from bosonization [29–31] provide an expression for the large distance behavior of the density matrix for any values of the interaction strengths [24,32]. In this case, the density matrix is written in terms of the dimensionless parameter called the Luttinger parameter, which for the Lieb-Liniger model reads $K = v_F/s$, where $v_F = \hbar\pi n/m$ is the Fermi velocity and s is the sound velocity of the Lieb-Liniger gas, which depends on γ and can be obtained via Bethe ansatz [21,33]. At leading order, the large distance asymptotic of the 1BDM reads

$$\frac{\rho(r)}{n} \simeq \frac{B_0}{(nr)^{1/2K}}, \quad (16)$$

where B_0 is a numerical prefactor [34]. Symmetrizing its expression in order to retrieve periodic boundary conditions, and

then performing the integral between 0 and L , we get access to the dimensionless momentum distribution peak scaling

$$\frac{n(k=0)}{L} = \frac{n^{1-1/2K} B_0}{2\pi} \left[\int_0^{L/2} \frac{dr}{r^{1/2K}} + \int_{L/2}^L \frac{dr}{(L-r)^{1/2K}} \right] \propto N^{1-1/2K}, \quad (17)$$

which implies

$$\mathcal{C}_0(T=0, \gamma) = 1 - \frac{1}{2K(\gamma)}, \quad (18)$$

in agreement with Ref. [16]. We verified that Eq. (17) also holds also if we symmetrize the density matrix according to the formula

$$\rho(r) \simeq \frac{n^{1-1/2K} B_0}{\left[\frac{L}{\pi} \sin\left(\frac{\pi x}{L}\right) \right]^{1/2K}}. \quad (19)$$

Notice that $\mathcal{C}_0(T=0, \gamma)$ depends only on γ through the Luttinger parameter, i.e., it depends on the ratio c/n and not on the interaction strength and the density separately. The power $\mathcal{C}_0(T=0, \gamma)$ varies between 1 for $\gamma \rightarrow 0$, to the value 1/2 obtained for the Tonks-Girardeau gas [35–37]. For very small values of the interaction parameter, say $\gamma \approx 10^{-4}$, one gets $\mathcal{C}_0 \approx 0.99$, which is very close to unity. Therefore the condensate fraction, λ_0/N , for a finite number of particles can be large and this could be seen in experiments with Rb atoms (when this occurs, one can say it is in the presence of a mesoscopic condensate).

Since λ_0 scales less than linearly with N and at the same time we should have $\sum_k \lambda_k = N$, in principle we could expect that at least for small values of k there may exist some $\mathcal{C}_{k \neq 0}$ different from zero. However, as we are going to show in the following, this is not the case in the thermodynamic limit. To obtain the behavior of the momentum distribution at nonzero momenta, we have to perform the Fourier transform, for which we get

$$\frac{n(k)}{L} \propto \int_0^{L/2} \frac{e^{ikr}}{r^{1/2K}} dr + \int_{L/2}^L \frac{e^{ikr}}{(L-r)^{1/2K}} dr \propto L^{1-1/2K} {}_1F_2\left(\frac{1}{2} - \frac{1}{4K}; \frac{1}{2}, \frac{3}{2} - \frac{1}{4K}; -\frac{\pi^2 l^2}{4}\right),$$

where ${}_1F_2(a; b_1, b_2; c)$ is the generalized hypergeometric function and we used the fact that $kL = 2\pi l$ with $l \in \mathbb{N}$. Expanding the hypergeometric function for large l and keeping only the leading term, we obtain

$$\frac{n(k)}{L} \propto L^{1-1/2K} l^{-1+1/2K} \propto N^0, \quad (20)$$

where in the last equality we used the fact that l needs to grow like L in the thermodynamic limit in order to have a fixed finite momentum k . Therefore the power $\mathcal{C}_{k \neq 0}$ for the one-dimensional gas at zero temperature and any interaction strength is simply vanishing,

$$\mathcal{C}_{k \neq 0}(T=0, \gamma) = 0, \quad (21)$$

and there is no quasi-fragmentation of the mesoscopic condensate. The same result can be found also using Eq. (19).

In Ref. [16] it was verified that the largest eigenvalue of the density matrix indeed scales with the exponent in Eq. (18)

by directly computing $\rho(r)$ using an interpolation method, which allows one to get a simple expression for the density matrix valid at any distance and interaction strengths. The power-law scaling shows very good agreement, confirming that the method sketched above to get access to the power \mathcal{C} is correct. We have then used the same interpolation scheme to get access to the N dependence of the $k \neq 0$ eigenvalues of the 1BDM [38]. Apart from oscillations at small particle numbers arising from a competition between the growth of l and L , for very large values of N the eigenvalues $\lambda_{k \neq 0}$ saturate and the power $\mathcal{C}_{k \neq 0}$ is indeed vanishing, confirming our prediction.

In the finite-temperature ($T \neq 0$) case, several results are available for the asymptotic behavior of the density matrix of the Lieb-Liniger gas [39–41]. In Ref. [41] an expression for the 1BDM as a sum of exponential functions is given in the form

$$\frac{\rho(r)}{n} = \sum_i \bar{B}_i e^{-r/\xi[\bar{v}_i]}, \quad (22)$$

where \bar{B}_i are distance independent amplitudes and $\xi[\bar{v}_i]$ the correlation length (shown to be always positive), depending on the temperature-dependent functions \bar{v}_i defined in Ref. [41], where it is also shown that the result in Eq. (22) reduces to Eq. (16) in the $T = 0$ case, as it should. We may now take the Fourier transform of the symmetrized version of Eq. (22), and obtain

$$\begin{aligned} \frac{n(k)}{L} &= \frac{1}{2\pi} \sum_i \bar{B}_i \left(\int_0^{L/2} e^{-r/\xi[\bar{v}_i]} dr + \int_{L/2}^L e^{-(L-r)/\xi[\bar{v}_i]} dr \right) \\ &\propto e^{-L/\xi[\bar{v}_i]}, \end{aligned}$$

where the last proportionality is valid both at zero and nonzero momentum k . Since $L = N/n$, analyzing the N leading dependence only, we have that for $N \rightarrow \infty$ the dimensionless momentum distribution is just a constant for any k , leading to the finite-temperature result:

$$\mathcal{C}_k(T \neq 0, \gamma) = 0, \quad (23)$$

which indicates complete absence of ordering.

In Fig. 2 we summarize the behavior of the exponent \mathcal{C}_0 for a homogeneous one-dimensional Bose gas for different temperatures. An inset shows the relation between \mathcal{C}_0 and the interaction parameter γ in the zero-temperature case, i.e., Eq. (18).

V. TWO DIMENSIONS

Properties of two-dimensional systems stand on their own and are between those of 1D, where \mathcal{C}_0 vanishes at finite temperature, and of 3D models, where $\mathcal{C}_0 = 1$ below the BEC critical temperature. As discussed in the Introduction, no ordinary phase transition takes place in 2D, due to the lack of ODLRO. However, 2D systems often feature the BKT topological phase transition named after Berezinskii, Kosterlitz, and Thouless who first discussed it in the two-dimensional XY model [42–44]. This transition is related to the presence of vortex and antivortex spin configurations at finite temperatures. At low T , below the BKT temperature T_{BKT} , vortex and antivortex pairs with vanishing total winding numbers

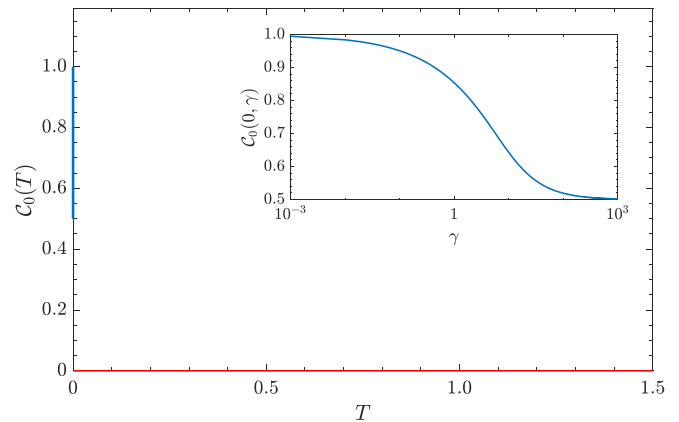


FIG. 2. Exponent $\mathcal{C}_0(T)$ with which the largest eigenvalue of the 1BDM of a homogeneous one-dimensional Bose gas scales with respect to the total number of particles N at different temperatures. Only for $T = 0$ does one have that \mathcal{C}_0 is nonvanishing and depends on the dimensionless interaction parameter γ via (18), as shown in the inset.

(neutrality condition) are present in the system and the correlation function between two distant spins decay as power law, indicating a phase with quasi-long-range order, also called BKT phase.

A simple estimate of T_{BKT} in the XY model is the Peierls value $T_{\text{BKT}} = \frac{\pi J}{2k_B}$ [45], where J is the interaction strength among the spins. In the low-temperature BKT regime the only relevant configurations are the spin waves, and the spin-wave approximation shall describe the system properly. As the temperature increases, the presence of free vortices with non-vanishing winding numbers becomes energetically favored, and, therefore, vortices and antivortices may unbind from each other. For temperatures above T_{BKT} , the presence of such topological excitations destroys the quasi-long-range order and the correlation functions become exponentially decaying [45–47]. An important statistical model used to approximatively describe the two-dimensional XY model is the one proposed by Villain [45,48]. While in the XY model the spin waves interact with the vortices, in the Villain model the spin waves are decoupled from the vortices degrees of freedom, making its Hamiltonian simply quadratic. Both models have the same topological characteristics and they belong to the same universality class, as one can see from the critical behavior of the anomalous dimension η of the two systems. The Villain model well describes the low-temperature phase of the XY model, since the Hamiltonian is essentially constituted by two decoupled harmonic oscillator terms; one for the spin waves and one for the vortices. Notice that the Villain model can be used both as a model *per se* and also as a convenient way to approximate the XY model [49].

Let us pause here to comment on the qualitative similarity of the low-dimensional ($D = 1$ and $D = 2$) systems studied in this work. In the thermodynamic limit at low temperatures, both for the one- and the two-dimensional cases, the systems can be described by field-theoretical models with Hamiltonians made up of two decoupled harmonic oscillator terms. These quadratic Hamiltonians are the Luttinger liquid and the Villain Hamiltonian for the one- and two-dimensional cases,

respectively. Therefore bosonization in $D = 1$ systems plays to a certain extent a similar role as the spin-wave approximation in $D = 2$ systems, both of them describing systems with quasi-long-range order in the low-temperature phase and the absence of order above their critical temperatures (which is vanishing in $D = 1$). Nevertheless, the phase transitions that characterize the models are for short-range models intrinsically different in the one- and two-dimensional cases. In $D = 2$ this phase transition is related to the formation of single independent topological excitations, which cannot happen in $D = 1$ geometries. Moreover in one dimension there is no phase transition at all at finite T , since the quasi-long-range order is limited to the zero-temperature limit.

Let us analyze the BKT phase transition in terms of the exponent \mathcal{C}_0 . At the BKT critical point the two-point correlation function scales as [50]

$$\rho(r) \sim \frac{1}{r^{D-2+\eta}}, \quad (24)$$

where η is the anomalous dimension critical exponent, that depends on the system under consideration. What is universal is the value at $T = 0$, for which $\eta(T = 0) = 0$, and that at $T = T_{\text{BKT}}$, which is given by $\eta(T = T_{\text{BKT}}) = 1/4$ [51]. The behavior of η between 0 and T_{BKT} is not universal.

From the knowledge of the behavior of the anomalous dimension—that will be discussed below—one can find an expression for the power \mathcal{C}_0 with which the dimensionless momentum distribution peak scales. One has

$$\frac{n(k=0)}{L^2} = \frac{1}{2\pi} \lim_{L \rightarrow \infty} \left[\int_0^{L/2} \frac{dr}{r^{\eta-1}} + \int_{L/2}^L \frac{dr}{(L-r)^{\eta-1}} \right],$$

$$\propto L^{2-\eta}, \quad (25)$$

where we symmetrized the density matrix in Eq. (24) in the radial coordinate variable r , passing to polar coordinates and performing the trivial integration over the azimuth angle. Since fixing the density $n = \frac{N}{L^2}$ in the large particle number limit implies that $L \propto \sqrt{N}$, we can then extract the power $\mathcal{C}_0(T/T_{\text{BKT}})$ with which the largest eigenvalue of the 1BDM scales, and it reads

$$\mathcal{C}_0 = 1 - \frac{\eta}{2}. \quad (26)$$

Notice that for the XY and Villain models the condensate fraction $\frac{\lambda_0}{N}$ is the magnetization density of the spin system and therefore Penrose-Onsager ODLRO manifests in a complete magnetization of the system, while having $\mathcal{C}_0 = 0$ is equivalent to saying that there exist no correlation and order between the spin variables.

Since the value of the anomalous dimension for such systems at the critical temperature is equal to $1/4$, one has

$$\mathcal{C}_0(T = T_{\text{BKT}}) = \frac{7}{8}, \quad (27)$$

and \mathcal{C}_0 jumps to zero for $T > T_{\text{BKT}}$, reflecting the universal jump for the superfluid stiffness [51]. A study of small corrections (found to be $\approx 0.02\%$) to the Nelson-Kosterlitz jump of the superfluid stiffness is in Refs. [52,53]. Using spin-wave approximation, one finds that at $T = 0$ there is ODLRO and therefore $\mathcal{C}_0(0) = 1$. Notice that at $T = 0$ ODLRO is allowed

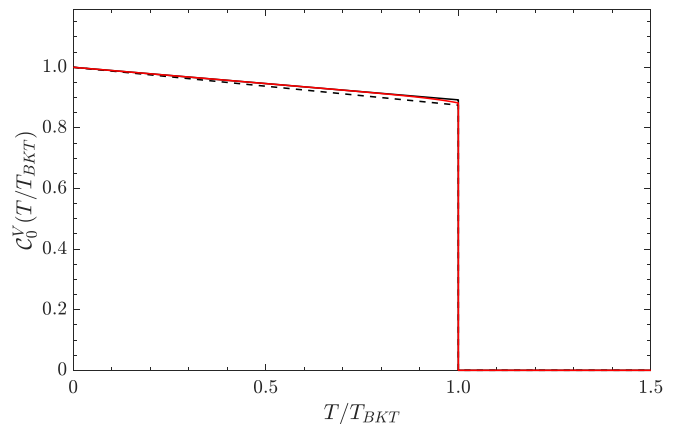


FIG. 3. $\mathcal{C}_0^V(T/T_{\text{BKT}})$ vs T/T_{BKT} for the Villain square lattice model. The red intermediate solid line represents the predicted value for \mathcal{C}_0 using Eq. (30) in Eq. (26), while the black solid and dashed lines represent, respectively, the low-temperature behaviors given respectively by Eqs. (31) and (32).

because there is no entropy contribution to the free energy of the system and the Mermin-Wagner theorem does not apply.

A. Villain model

In the case of the square lattice planar Villain model, one expects that the anomalous dimension should be of the form $\eta_V \simeq \frac{k_B T}{2\pi A}$ at low temperatures, since the theory is quadratic and the spin-wave approximation shall apply everywhere, in particular very close to the critical point, where vortex configurations become relevant. Using as definition for the partition function of the Villain model the standard one given, e.g., in [54], the value for A will be provided in the following. Villain [48] proposed a correction term to account for vortex contributions to the anomalous dimension close to the critical point. Assuming that the interaction between the vortices can be neglected, this correction yields [48]

$$\eta_V = \frac{k_B T}{2\pi A} + \pi^2 k_B T \frac{e^{-\pi^2 A/k_B T}}{\pi A - 2k_B T}. \quad (28)$$

Using the BKT renormalization group flow equations, the value for the critical temperature of the Villain models is found to be [54]

$$\frac{k_B T_{\text{BKT}}}{A} = \frac{1}{0.74} \simeq 1.351, \quad (29)$$

in agreement with the result obtained from the high-precision Monte Carlo simulation performed in Ref. [54] up to $L = 512$ lattice sites. Substituting Eq. (29) into Eq. (28), we have an estimate for the behavior of the anomalous dimension of the square lattice Villain model in terms of the dimensionless ratio T/T_{BKT} , which reads

$$\eta_V(T/T_{\text{BKT}}) = \mathcal{A} \frac{T}{T_{\text{BKT}}} + \frac{\pi^2}{2} \frac{e^{-\mathcal{B} T_{\text{BKT}}/T}}{(-1 + \mathcal{D} \frac{T_{\text{BKT}}}{T})}, \quad (30)$$

where $\mathcal{A} \approx 0.215$, $\mathcal{B} \approx 7.304$, and $\mathcal{D} \approx 1.162$.

Introducing Eq. (30) into Eq. (26), one obtains the results plotted as the red intermediate solid line in Fig. 3. Notice that according to the approximation in Eq. (28), one has $\eta_V(T =$

$T_{\text{BKT}} \simeq 0.236$, i.e., $C_0^V(1) = 0.882$, with “V” referring to the Villain model. This result differs from the one coming from Monte Carlo simulations [54], $\eta_V = 0.2495 \pm 0.0006$, for about 5%. Low-temperature predictions for the exponent $C_0^V(T)$ may be formulated in two ways:

(1) Disregarding the second term in the right-hand side of Eq. (28), which may be safely neglected in the low-temperature regime at $T \ll T_{\text{BKT}}$ [48], which yields, via Eq. (26),

$$C_0^V(T/T_{\text{BKT}}) \simeq 1 - \frac{1}{2} \left(\frac{T}{2\pi T_{\text{BKT}}} \frac{1}{0.74} \right) \quad (31)$$

with T_{BKT} obtained by Monte Carlo simulations [see Eq. (29)].

(2) Using the Peierls argument $\frac{k_B T_{\text{BKT}}}{A} = \frac{\pi}{2}$, one has

$$C_0^V(T/T_{\text{BKT}}) \simeq 1 - \frac{1}{2} \left(\frac{T}{T_{\text{BKT}}} \frac{1}{4} \right). \quad (32)$$

These two behaviors are reported as black solid and dashed lines, respectively, in Fig. 3. Notice from the plot that the low- T behavior of Eq. (31) is good even in regions close to T_{BKT} , where the corrective term introduced by Villain starts to play a role. The predictions of (32), which at variance do not take into account the effect of vortices, do not match with the same accuracy with the expected results already from $T \approx 0.5T_{\text{BKT}}$.

B. XY model

For the two-dimensional classical XY model, whose Hamiltonian reads $H = -J \sum_{i,j} \cos(\phi_i - \phi_j)$ (with the sum on nearest neighbour sites), the critical temperature has been evaluated using Monte Carlo techniques obtaining [55–58]

$$\frac{k_B T_{\text{BKT}}}{J} = 0.893 \pm 0.001, \quad (33)$$

while recent approximate, semianalytical, functional renormalization group (FRG) results give $k_B T_{\text{BKT}} = (0.94 \pm 0.02)J$ [59]. The anomalous dimension is found to be equal to

$$\eta_{XY} = \frac{k_B T}{2\pi J_s(T)},$$

where $J_s(T)$ is the superfluid (or spin) stiffness of the model, and has been recently calculated for the XY model in a square lattice in Ref. [60] using simulations up to 256 lattice sites.

Therefore we may now compute the $k = 0$ Fourier transform of the spin-spin correlation function as in Eq. (25). From Eq. (26), one has

$$C_0^{XY}(T) = 1 - \frac{\eta_{XY}}{2}. \quad (34)$$

Using the Villain approximation we can obtain an expression for the behavior of the anomalous dimension for the XY model. The Villain approximation, indeed, is based on the fact that there exist a (nonexact) map between the interaction parameter A and the spin-spin interaction parameter J , which relates the Villain Hamiltonian to the XY model [48]. This mapping reads

$$\frac{A}{k_B T} = -\frac{1}{2} \left\{ \ln \left[\frac{I_1\left(\frac{J}{k_B T}\right)}{I_0\left(\frac{J}{k_B T}\right)} \right] \right\}^{-1}, \quad (35)$$

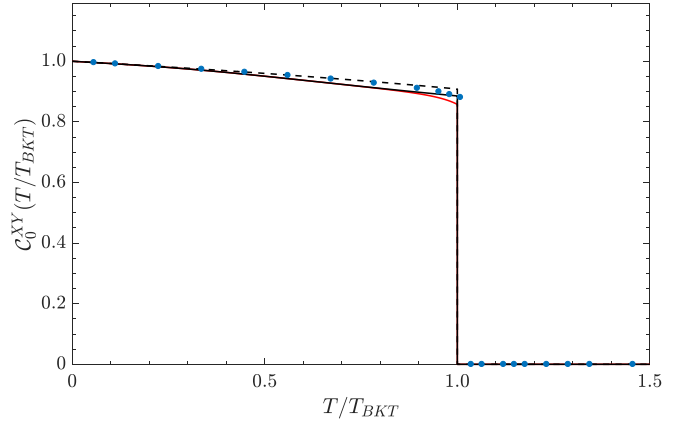


FIG. 4. $C_0^{XY}(T/T_{\text{BKT}})$ vs T/T_{BKT} . Blue points are the numerical values of C_0 obtained from Eq. (34) with anomalous dimension $\eta_{XY} = \frac{T}{2\pi J_s(T)}$ and using the superfluid stiffness results of Ref. [60]. The universal jump from $C_0(T_{\text{BKT}}) = \frac{7}{8}$ to $C_0(T > T_{\text{BKT}}) = 0$ is evident. The bottom red solid line comes from the Villain prediction Eq. (36). Finally the black solid and dashed lines represent the low-temperature predictions of Eqs. (37) and (38), respectively.

where $I_n(x)$ are the modified Bessel functions of the first kind of degree n . We may therefore substitute this expression into the approximation given in Eq. (28). We find

$$\eta_{XY} = -\frac{1}{\pi} \ln \left[\frac{I_1\left(\frac{J}{k_B T}\right)}{I_0\left(\frac{J}{k_B T}\right)} \right] + \frac{\pi^2}{2} e^{(\pi^2/2)\{\ln[I_1(\frac{J}{k_B T})/I_0(\frac{J}{k_B T})]\}^{-1}} \times \left\{ -1 + \frac{\pi}{\pi + 4 \ln \left[I_1\left(\frac{J}{k_B T}\right) \right] - 4 \ln \left[I_0\left(\frac{J}{k_B T}\right) \right]} \right\}. \quad (36)$$

Using the mapping of Eq. (35), the Monte Carlo results of Ref. [54] for the critical temperature of the Villain model, i.e., Eq. (29), translates into

$$\frac{k_B T_{\text{BKT}}}{J} = 0.842,$$

which is pretty close to the Monte Carlo results of Refs. [55–58] reported in Eq. (33). The equation which relates A to J seems then to be reliable within a $\approx 6\%$ accuracy even very close to the critical point.

Similarly to what we have done for the Villain model, a low-temperature prediction can be made by neglecting the second term in the right-hand side of Eq. (36). Using Eq. (34) we get

$$C_0^{XY}(T) \simeq 1 + \frac{1}{2\pi} \ln \left[\frac{I_1\left(\frac{J}{k_B T}\right)}{I_0\left(\frac{J}{k_B T}\right)} \right]. \quad (37)$$

On the other hand, one can also employ the low-temperature expansion results: $\frac{J_s(T)}{J} \simeq 1 - \frac{k_B T}{4J}$, which is known to be consistent with several approaches, such as self-consistent harmonic approximation [61], Monte Carlo simulations [62], and FRG [59]. This procedure leads to the expression

$$C_0^{XY}(T/T_{\text{BKT}}) \simeq 1 - \frac{1}{\pi} \frac{T/T_{\text{BKT}}}{\frac{4J}{k_B T_{\text{BKT}}} - T/T_{\text{BKT}}}. \quad (38)$$

In Fig. 4 we report as blue points the behavior of (34) for $\eta_{XY} = \frac{k_B T}{2\pi J_s(T)}$ with respect to the dimensionless quantity T/T_{BKT} obtained using the results of Ref. [60]. The bottom red solid line represents the Villain approximation prediction given in Eq. (36) with T_{BKT} given by Eq. (33), while the black solid and dashed lines represent the low-temperature behaviors in Eqs. (37) and (38), respectively. Figure 4 confirms the validity of the low-temperature expansion in Eq. (38) in the range $T \in [0, 0.8T_{\text{BKT}}]$, while Eq. (38) remains reliable up to T_{BKT} .

C. Bose gas

Under certain conditions a two-dimensional Bose gas can be mapped onto the XY model and from this mapping one can derive the decay of correlation functions and the ordering type of the bosonic system [63–66]. Indeed, when density fluctuations are strongly suppressed the effective low-energy Hamiltonian of a two-dimensional Bose gas is equivalent to the continuous version of the Hamiltonian of the XY model on the lattice. The BKT phase of the XY model corresponds then to the superfluid state of the Bose gas and quasi-long-range order is present. Above the critical temperature the normal state appears and superfluidity breaks down. This abrupt change of phase is characterized by a universal jump of the superfluid density (stiffness), which switches between its low-temperature value $\rho_s = \frac{2m^2 k_B T}{\pi \hbar^2}$ to $\rho_s = 0$ for $T > T_{\text{BKT}}$ [51,52].

In Refs. [67,68] it has been shown that the asymptotic behavior of the 1BDM of a two-dimensional weakly interacting Bose gas at finite temperatures scales as

$$\rho(r) \sim \frac{1}{r^{m^2 k_B T / 2\pi \hbar^2 \rho_s}}, \quad (39)$$

where ρ_s is the superfluid density of the gas. The superfluid density of the system assumes the form [64]

$$\rho_s = \frac{2m^2 k_B T}{\hbar^2 \pi} f(X), \quad (40)$$

where $X = \frac{\hbar^2(\mu - \mu_c)}{m k_B T U}$ measures the distance from the critical point, with μ the chemical potential and the critical value μ_c given by

$$\mu_c = \frac{m k_B T U}{\hbar^2 \pi} \ln \left(\frac{\hbar^2 \xi_\mu}{m U} \right). \quad (41)$$

The function $f(X)$ in Eq. (40) is a dimensionless universal function, which has been numerically determined in Ref. [64]. The variable U appearing in X is the interparticle interaction strength, so that $\frac{mU}{\hbar^2} \ll 1$ and $X \gg 1$ correspond to the weakly interacting limit, while the constant ξ_μ appearing in Eq. (41) is given by $\xi_\mu = 13.2 \pm 0.2$ [64].

Applying the same procedure used for the Villain and the XY models, we obtain the following exponent \mathcal{C}_0 for the scaling of the dimensionless momentum distribution peak with respect to the number of particles of the two-dimensional Bose gas:

$$\mathcal{C}_0^{\text{Bose}}(X) = 1 - \frac{1}{8f(X)}. \quad (42)$$

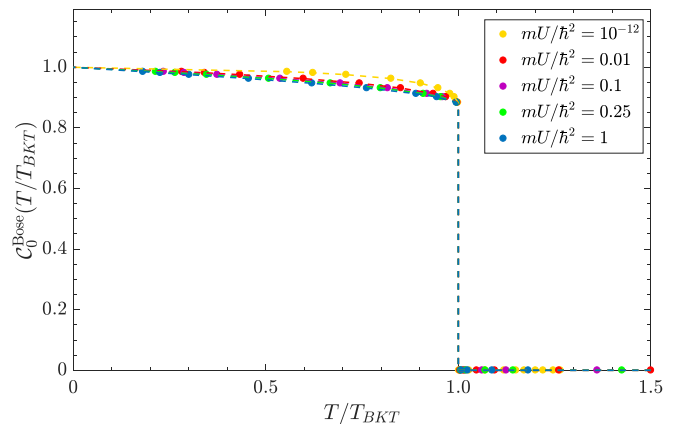


FIG. 5. $\mathcal{C}_0^{\text{Bose}}(T/T_{\text{BKT}})$ vs T/T_{BKT} for different interactions $\frac{mU}{\hbar^2}$. Points are the numerical value of \mathcal{C}_0 obtained from numerical simulations performed in Ref. [64], while dashed lines are drawn as a guide for the eyes. In each case the universal jump from $\mathcal{C}_0(T_{\text{BKT}}) = \frac{7}{8}$ to $\mathcal{C}_0(T > T_{\text{BKT}}) = 0$ is evident.

The jump of the superfluid stiffness ρ_s at criticality implies that $f(X)$ will jump from 0 to 1 at $X = 0$, i.e., at the critical point. Therefore, the exponent \mathcal{C}_0 will jump from the universal value $\frac{7}{8}$ to 0 at the critical BKT temperature. The relation between the exponent \mathcal{C}_0 and the ratio T/T_{BKT} is constructed from the expression [64]

$$\frac{T}{T_{\text{BKT}}}(X) = \frac{1}{1 + 2\pi \lambda(X) / \ln(\hbar^2 \xi / mU)}, \quad (43)$$

where $\lambda(X) = [X + \theta(X) - \theta_0]/2$ with $\theta(X)$ found via numerical simulations for system sizes up to 512 in Ref. [64]. The (nonperturbative) constant ξ in Eq. (43) is given by [64]

$$\xi = 380 \pm 3, \quad (44)$$

and $\theta_0 = \frac{1}{\pi} \ln(\frac{\xi}{\xi_\mu})$ is then found to be $\theta = 1.07 \pm 0.01$.

Knowing the relation between T/T_{BKT} and X and the relation between $\mathcal{C}_0^{\text{Bose}}$ and X , we can then track down the dependence of the exponent \mathcal{C}_0 with which the dimensionless momentum distribution peak scales with the number of particles N for different temperatures. We report its behavior in Fig. 5 for different values of the interaction U .

An important comment about Fig. 5 is that in the limit of the dimensionless interaction parameter $\frac{mU}{\hbar^2} \rightarrow 0$, the exponent \mathcal{C}_0 tends to be closer (with respect to higher values of U) to the unity up to temperatures closer to T_{BKT} . In other words, the smaller is U , the closer to 1 is \mathcal{C}_0 at fixed $T/T_{\text{BKT}} < 1$. Going even closer to T_{BKT} from below, the decrease to the value $\frac{7}{8}$ happens abruptly for $\frac{mU}{\hbar^2} \simeq 0$ at $T \simeq T_{\text{BKT}}$. Since \mathcal{C}_0 has to be $7/8$ at $T = T_{\text{BKT}}$, this is associated to a kind of *double jump* occurring for $T \rightarrow T_{\text{BKT}}^-$ for $U \rightarrow 0$, since in this limit \mathcal{C}_0 reaches a value different from (and larger than) $7/8$ coming from low-temperature/large- X expansion that we are going to shortly introduce, then it abruptly jumps from this value to $7/8$ and then jumps from $7/8$ to 0. More comments on the double jump occurrence are below.

Finally, it is worth noting that the values for $\frac{mU}{\hbar^2} = 1$, reported in Fig. 5, are out of the validity range for the weak interacting gas. Then, the mean-field arguments of Ref. [64]

cannot be applied anymore, and one should take into account quantum fluctuations.

Low-temperature predictions may also be formulated, similarly to what we did for the Villain and XY models, but with some subtleties to be worked out. In the low- T regime (i.e., far from the critical point), it is $X \rightarrow \infty$ and the function $\theta(X)$ satisfies [64]

$$\theta(X) - \frac{1}{\pi} \ln \theta(X) = X + \frac{1}{\pi} \ln(2\xi_\mu), \quad (45)$$

which is a transcendental equation admitting two values for θ for a single value of X . These two solutions can be distinguished in terms of the behavior of $\theta(X)$ for $X \rightarrow \infty$. The first set is the one having a vanishing value of $\theta(X \rightarrow \infty)$ and it is given by

$$\theta(X \rightarrow \infty) = \frac{e^{-\pi X}}{2\xi_\mu}, \quad (46)$$

which is the solution of $-\frac{1}{\pi} \ln \theta(X) = X + \frac{1}{\pi} \ln(2\xi_\mu)$ as well as a solution of Eq. (45) for $X \rightarrow \infty$. This first set is not interesting for us and we look for a function $\theta(X)$ which diverges for large X . This represents the second set of solutions and one has

$$\theta^{(0)}(X \rightarrow \infty) = X + \frac{1}{\pi} \ln(2\xi_\mu), \quad (47)$$

which is the zeroth-order solution of Eq. (45) without the logarithmic term in the left-hand side. In the low- T regime one may also write [64]

$$f^{(0)}(X \rightarrow \infty) = \frac{\pi}{2} \theta^{(0)}(X) - \frac{1}{4} = \frac{2\pi X + 2 \ln(2\xi_\mu) - 1}{4}, \quad (48)$$

where the last identity follows from Eq. (47). Reminding one that $\lambda(X) = [X + \theta(X) - \theta_0]/2$ and using Eq. (47), one has an expression also for the $\lambda(X)$ function in the low-temperature regime at the zeroth order of approximation:

$$\lambda^{(0)}(X \rightarrow \infty) = X + \frac{1}{2\pi} \ln \left[\frac{2(\xi_\mu)^2}{\xi} \right]. \quad (49)$$

Therefore, substituting into Eq. (43), one can write an expression for X (at the zeroth order in terms of the variable T/T_{BKT}) reading

$$X^{(0)} = -\frac{1}{2\pi} \ln \left[\frac{2(\xi_\mu)^2}{\xi} \right] + \frac{1}{2\pi} \ln \left(\frac{\hbar^2 \xi}{mU} \right) \left(\frac{T_{\text{BKT}}}{T} - 1 \right). \quad (50)$$

Finally, inserting Eq. (50) into Eq. (48), we may substitute the equation for $f^{(0)}(X \rightarrow \infty)$ into Eq. (42) to obtain an analytical expression for the exponent C_0^{Bose} at low temperatures:

$$C_0^{\text{Bose}^{(0)}}(T/T_{\text{BKT}}) \simeq 1 + \frac{1}{2} \left[1 - \ln(2\xi) - \ln \left(\frac{\hbar^2 \xi}{mU} \right) \left(\frac{T_{\text{BKT}}}{T} - 1 \right) \right]^{-1}, \quad (51)$$

where the superscript (0) denotes we are at the lowest order in the considered approximation. One can obtain higher-order solutions by substituting the expression in Eq. (47) in the

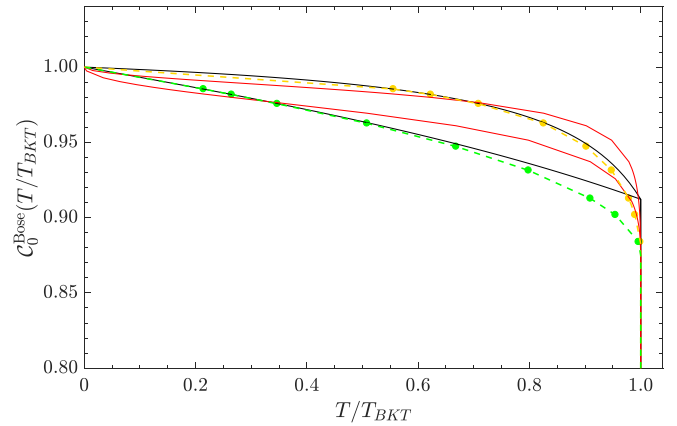


FIG. 6. Comparison of low-temperature predictions for $C_0^{\text{Bose}}(T/T_{\text{BKT}})$ vs T/T_{BKT} with numerical results for the two different interactions $\frac{mU}{\hbar^2} = 10^{-12}$, 0.25. Bottom green (top yellow) points are the numerical values from numerical simulations performed in [64], respectively, for $\frac{mU}{\hbar^2} = 0.25$ ($\frac{mU}{\hbar^2} = 10^{-12}$), while dashed lines are drawn as a guide for the eye. Low-temperature predictions from third-order approximation are reported in black solid lines for two different interaction strengths: the line below (above) is for $\frac{mU}{\hbar^2} = 0.25$ ($\frac{mU}{\hbar^2} = 10^{-12}$). Red solid lines (standing above the black ones for both interaction strengths) represent the predictions for $T \simeq T_{\text{BKT}}$ from Eq. (62).

logarithmic term of the Eq. (45) and solve for $\theta(X)$, which will now be the solution at the first order of approximation, i.e., it reads

$$\theta^{(1)}(X) = X + \frac{1}{\pi} \ln(2\xi_\mu) + \frac{1}{\pi} \ln \theta^{(0)}(X). \quad (52)$$

Following the same procedure sketched above for the zeroth-order case, we obtained the following analytical form for C_0^{Bose} at low temperatures at first-order approximation:

$$C_0^{\text{Bose}^{(1)}}(T/T_{\text{BKT}}) \simeq 1 + \frac{1}{2} \left\{ 1 - 2 \ln \left[\frac{2mU}{\hbar^2} \left(\frac{\hbar^2 \xi}{2mU} \right)^{T_{\text{BKT}}/T} \right] + W \left(\frac{4\pi mU}{\hbar^2} \left(\frac{\hbar^2 \xi}{2mU} \right)^{T_{\text{BKT}}/T} \right) \right\}^{-1}, \quad (53)$$

where $W(z)$ is the Lambert or product logarithm function. Higher-order solutions may be obtained following the same recipe, but from the second-order case is not possible to write an analytical expression for X in terms of T/T_{BKT} . Therefore, one can work out only the numerics in order to obtain the low-temperature behavior of the exponent $C_0^{\text{Bose}(j \geq 2)}(T/T_{\text{BKT}})$. In the present work the third-order approximation has been also investigated, but we envisage no particular difficulty in going beyond.

In Fig. 6 we report the comparison between the low-temperature expansions with the values for C_0^{Bose} obtained from the numerical Monte Carlo results of Ref. [64] in the very small interaction limit $\frac{mU}{\hbar^2} = 10^{-12}$, and for the intermediate interaction case $\frac{mU}{\hbar^2} = 0.25$. The agreement is good up

to 3% even for $T = T_{\text{BKT}}$, where

$$C_0^{\text{Bose}(3)}(1) \simeq 0.912, \quad (54)$$

independently of the interaction parameter. It is important to notice that for smaller values of U the low-temperature predictions for the exponent C_0^{Bose} are valid for a larger range of temperatures, since for very weak interactions the variable X is very large even at $T \approx T_{\text{BKT}}$. So, decreasing U the range of validity of the low-temperature predictions increase up to a value which becomes increasingly close to T_{BKT} . Indeed, for $\frac{mU}{\hbar^2} = 10^{-12}$ the low- T prediction remains reliable up to $T \approx 0.9T_{\text{BKT}}$.

This implies that for $U \rightarrow 0$, and in practice $\frac{mU}{\hbar^2}$ extremely small, there will be the above-mentioned double jump phenomenon for the exponent C_0^{Bose} which will pass near below T_{BKT} from a value close to the quantity in Eq. (54), 0.912, to $\frac{7}{8} = 0.875$ for $T = T_{\text{BKT}}$. Then the second Nelson-Kosterlitz jump will lead C_0^{Bose} to pass from $7/8$ to zero. It can be seen that there is not appreciable change in this result if one goes to higher orders of approximation. Despite being not too large in absolute value, the first jump should be appreciable in experiments or simulations, one problem being that one has to go possibly to very small values of $\frac{mU}{\hbar^2}$. We observe that the prediction of the double jump is based on the validity of the low- T expansion and its extension near T_{BKT} for U very small, and when T is scaled in units of T_{BKT} , which in turn depends on U . Therefore it could be that further corrections near T_{BKT} may soften the first jump, making it a very steep decrease. Notice, that due to Eq. (26), the value $C_0 = 0.912$ corresponds to $\eta = 0.176$, which is pretty far from the universal value $\eta = 0.25$, so that going to very small U one should appreciate such relatively large variation of η near T_{BKT} . Further simulations would be extremely useful to better quantify such steep decrease of η close to T_{BKT} .

Interestingly enough, at low temperatures, the Bose gas can be described by the corresponding results for the XY model. Therefore, posing $C_0^{XY} = C_0^{\text{Bose}(0)}$, i.e., equating the low-temperature result of the XY model in Eq. (38) to the low-temperature result for the 2D Bose gas in Eq. (51) for any rescaled temperature T/T_{BKT} , one obtains the following value for the parameter ξ :

$$\xi = \frac{1}{2}e^{1+(\pi/2)(T-1)}, \quad (55)$$

where $\mathcal{T} \equiv 4J/k_B T_{\text{BKT}}^{(XY)}$. When the dimensionless interaction strength satisfies the equation

$$\frac{mU}{\hbar^2} = \frac{1}{2}e^{1-(\pi/2)} = 0.283, \quad (56)$$

the low- T predictions in Eq. (51) equal Eq. (38), valid respectively for the 2D Bose gas and the XY model. Since for the XY model it is $k_B T_{\text{BKT}}^{(XY)}/J = 0.893 \pm 0.001$, one finds

$$\xi = 321 \pm 3, \quad (57)$$

which should be compared with the Monte Carlo result $\xi = 380 \pm 3$. The comparison shows that this result (that depends only on the critical temperature of the 2D XY model) is not entirely unreasonable, given the nonperturbative nature of the parameter ξ and the well-known failure of mean-field calculations to determine it and in general the difficulty of obtaining analytical estimates for it.

Predictions can be made also for $T \simeq T_{\text{BKT}}$, i.e., $X \rightarrow 0^+$. We write the function $\theta(X)$ as

$$\theta(X \rightarrow 0) = bX + \frac{1}{\pi} \ln \left(\frac{\xi}{\xi_\mu} \right), \quad (58)$$

where b is a constant to be determined by fitting the values of $\theta(X)$ for small X coming from Monte Carlo simulations with the law in Eq. (58). It is found $b = 1.29 \pm 0.05$.

For the function $f(X)$ is found instead [43,44,64]

$$f(X \rightarrow 0) = 1 + \sqrt{2\kappa'X}, \quad (59)$$

with $\kappa' = 0.61 \pm 0.01$. For $\lambda(X)$, from Eq. (58), is simply found that

$$\lambda(X \rightarrow 0) = \frac{b-1}{2}X, \quad (60)$$

and therefore, following the same reasoning of the low- T case, from Eq. (43) it follows that

$$X = \frac{\ln \left(\frac{\hbar^2 \xi}{mU} \right) \left(\frac{T_{\text{BKT}}}{T} - 1 \right)}{\pi(b-1)}. \quad (61)$$

Finally we can substitute the above expression for X into Eq. (59) and then into Eq. (42) to obtain an expression for C_0^{Bose} for $T \simeq T_{\text{BKT}}$ which reads

$$C_0^{\text{Bose}}(T \rightarrow T_{\text{BKT}}) \simeq 1 - \frac{1}{8} \left[1 + \sqrt{\frac{2\kappa'}{\pi(b-1)} \ln \left(\frac{\hbar^2 \xi}{mU} \right)} \times \left(\frac{T_{\text{BKT}}}{T} - 1 \right) \right]^{-1}. \quad (62)$$

We report its behavior in red solid lines in Fig. 6 along with numerical Monte Carlo results of C_0^{Bose} obtained from Ref. [64] for different interactions. The agreement is good only for values $X \simeq 0$ and the analytical prediction of Eq. (62) gets rapidly worse for decreasing temperatures.

Equating the two behaviours in Eqs. (51) and (62) we can find how the temperature with which the two curves intersect depends on the dimensionless interaction parameter $\frac{mU}{\hbar^2}$. Substituting this expression back to either (51) or (62), it is found that the value for C_0^{Bose} at which the two limiting behaviors intersect is independent on the interaction strength, and reads

$$\begin{aligned} C_0^{\text{Bose}(0)} &= 1 - \frac{1}{8} \left[1 + \sqrt{\frac{2\kappa'}{\pi(b-1)}} \sqrt{5 - \ln(2\xi) + \frac{16\kappa'}{\pi(b-1)}} \right. \\ &\quad \left. - 4 \sqrt{\frac{2\kappa'}{\pi(b-1)}} \sqrt{5 - \ln(2\xi) + \frac{8\kappa'}{\pi(b-1)}} \right]^{-1} \\ &\simeq 0.914. \end{aligned}$$

This intersection value can also be obtained using the first-order approximation formula $C_0^{\text{Bose}(1)}$, for which one gets 0.915.

Let us now study the scaling exponent $C_{k \neq 0}$ for the eigenvalues of the 1BDM corresponding to nonvanishing momenta. As in the previous section, we have to compute the Fourier

transform of the symmetrized asymptotic behavior of the density matrix, hence

$$\begin{aligned} \frac{n(k)}{L^2} &\propto \lim_{L \rightarrow \infty} \int_0^{2\pi} e^{ikr \cos(\theta)} d\theta \left[\int_0^{L/2} \frac{dr}{r^{\eta-1}} + \int_{L/2}^L \frac{dr}{(L-r)^{\eta-1}} \right] \\ &= \lim_{L \rightarrow \infty} \left[\int_0^{L/2} \frac{J_0(kr)}{r^{\eta-1}} dr + \int_{L/2}^L \frac{J_0(kr)}{(L-r)^{\eta-1}} dr \right], \end{aligned}$$

where we passed to polar coordinates symmetrizing on the radial component as was done for the XY model case, $J_0(x)$ is the Bessel function of the first kind, and $\eta = \frac{m^2 k_B T}{2\pi \hbar^2 \rho_s}$ for the weakly interacting Bose gas, while $\eta = \frac{T}{2\pi J_s(T)}$ for the XY model. Focusing only on the first half of the integration interval [69] we obtain

$$\frac{n(k)}{L^2} \propto L^{2-\eta} {}_1F_2\left(1 - \frac{\eta}{2}; 1, 2 - \frac{\eta}{2}; -\frac{\pi^2 l^2}{4}\right), \quad (63)$$

where we used $kL = 2\pi l$ with $l \in \mathbb{N}$. Expanding the hypergeometric function for large l and focusing only the leading term, we obtain finally

$$\frac{n(k)}{L^2} \propto L^{2-\eta} l^{\eta-2} \propto N^0, \quad (64)$$

where in the last proportion we wrote $l \propto L$ in order that k remains finite in the thermodynamic limit and $L \propto \sqrt{N}$, since the density $n = N/L^2$ is fixed. Therefore we simply have

$$C_{k \neq 0}(T) = 0, \quad (65)$$

both for the XY and the two-dimensional Bose gas systems for zero and finite temperatures.

VI. CONCLUSIONS

The goal of the present paper has been to characterize off-diagonal long-range order (ODLRO) properties of interacting bosons at finite temperatures through the study of the eigenvalues' scaling of the one-body density matrix (1BDM) vs the number of particles N . For translational invariant systems, denoting by λ_k the eigenvalues of the 1BDM and by λ_0 the largest among them, one can define the scaling exponents C_k from the relation $\lambda_k \sim N^{C_k}$. The exponents C_k depend on the temperature T and on the strength of the interaction (which we assume short ranged), and on the dimension D as well. According to the Penrose-Onsager criterion, $C_0 = 1$ corresponds to ODLRO, while at variance the opposite limit $C_0 = 0$ corresponds to the single-particle occupation of the natural orbital associated to λ_0 . The intermediate case, $0 < C_0 < 1$, is associated for translational invariant systems to the power-law decaying of nonconnected correlation functions and it can be seen as identifying quasi-long-range order.

After introducing some basic definitions and properties of the 1BDM, we discussed how to obtain the exponents C_k directly from the large distance behavior of the 1BDM. The ODLRO in the three-dimensional case for temperatures below the Bose-Einstein critical temperature has been described, as well as quasi-long-range order in the

one- and two-dimensional Bose gases for different interactions and temperatures, discussing the connection of the Mermin-Wagner theorem with the occurrence of mesoscopic condensation. We showed that in 1D it is $C_0 = 0$ for nonvanishing temperature, while in 3D it is $C_0 = 1$ ($C_0 = 0$) for temperatures smaller (larger) than the Bose-Einstein critical temperature. We then focused on the two-dimensional case. We presented the application of our methods to the XY and Villain models, where ODLRO is translated as a magnetization of the system, and to the 2D Bose gases. A universal jump of the power C_0 from $\frac{7}{8}$ to 0 is found at the Berezinskii-Kosterlitz-Thouless temperature T_{BKT} , reflecting the universal jump for the superfluid stiffness. The dependence of C_0 between $T = 0$ (at which $C_0 = 1$) and T_{BKT} is studied in the different models. We found a weak dependence of it when the reduced temperature T/T_{BKT} is used. An estimate for the (nonperturbative) parameter ξ entering the equation of state of the 2D Bose gases was obtained using low-temperature expansions and compared with the Monte Carlo result. We also unveiled a ‘‘double jump’’-like behavior for C_0 , and correspondingly of the anomalous dimension η , right below T_{BKT} in the limit of vanishing interactions. When the dimensionless parameter mU/\hbar^2 is very small, the validity region of the low-temperature expansion enlarges towards T_{BKT} as soon as mU/\hbar^2 decreases. When such regime is reached, then C_0 tends to the value ≈ 0.912 , and again moving towards T_{BKT} from below it abruptly (or, at least, in a very steep way) decreases to the universal value $7/8$, then jumping again to 0. We presented a detailed discussion of the weakly interacting regime and we commented how the double jump behavior could be appreciable for very low values of the parameter mU/\hbar^2 . Then we analyzed the behavior of $C_{k \neq 0}$, finding that in none of the cases presented is there quasi-fragmentation, i.e., $C_{k \neq 0} = 0$.

Our investigation is based both on the homogeneity of space and the thermodynamic limit, and therefore it will be interesting to study in a future work whether adding a confining external potential could change our predictions and how a finite number of particles affects the results. Moreover, it would be of interest to consider long-range interactions [70] and the presence of disorder, where rigorous results are available in literature [71,72]. We also mention that for 2D anyonic gases, despite the presence of considerable literature (see, e.g., [73–76], and references therein), to the best of our knowledge no results for the scaling exponents $C_k(T)$ are available to date.

Finally, we observe that for interacting fermions ODLRO is, of course, not present for the 1BDM, but it may exist for the 2BDM in the presence of attractions, so that it would be interesting to perform a parallel study to the one presented here for fermionic systems. In particular, in two-dimensional attractive Fermi gases at the BEC-BCS crossover, the scaling behavior of the 2BDM has been recently connected to the presence of quantum anomaly and the ODLRO analysis may clarify its relation to the finite temperature superfluid transition [78,79]. Moreover, the recently achieved direct measurements of momentum correlations in one-dimensional Fermi systems [80] would provide an excellent experimental counterpart to the study of ODLRO in these systems, where several theoretical evidences of dynamical critical scaling have been found [81–85].

ACKNOWLEDGMENTS

We thank T. Enss, L. Lepori, D. Lundholm, and I. Nandori for discussions and J. Yngvason and M. Hasenbusch for useful correspondence. A.T. acknowledges the kind hospitality at “Mathematical physics of anyons and topological states of matter,” taking place in Nordita, Stockholm (Sweden), March 2019, where parts of present work have been

fruitfully discussed with participants to the conference. This work is supported by the Deutsche Forschungsgemeinschaft (DFG, German Research Foundation) under Germany’s Excellence Strategy “EXC-2181/1-390900948” (the Heidelberg STRUCTURES Excellence Cluster). N.D. and A.T. acknowledge support from the CNR/MTA Italy-Hungary 2019–2021 Joint Project “Strongly interacting systems in confined geometries.”

-
- [1] O. Penrose and L. Onsager, *Phys. Rev.* **104**, 576 (1956).
 [2] P. W. Anderson, *Rev. Mod. Phys.* **38**, 298 (1966).
 [3] K. Huang, *Bose-Einstein Condensation and Superfluidity*, in [77], p. 31.
 [4] N. D. Mermin and H. Wagner, *Phys. Rev. Lett.* **17**, 1307 (1966).
 [5] P. C. Hohenberg, *Phys. Rev.* **158**, 383 (1967).
 [6] N. Defenu, P. Mati, I. G. Márián, I. Nándori, and A. Trombettoni, *J. High Energy Phys.* **05** (2015) 141.
 [7] N. Defenu, A. Trombettoni, and S. Ruffo, *Phys. Rev. B* **94**, 224411 (2016); **96**, 104432 (2017).
 [8] G. Gori, M. Michelangeli, N. Defenu, and A. Trombettoni, *Phys. Rev. E* **96**, 012108 (2017).
 [9] U. R. Fischer, *Phys. Rev. Lett.* **89**, 280402 (2002); *J. Low Temp. Phys.* **138**, 723 (2005).
 [10] L. P. Pitaevskii and S. Stringari, *Bose-Einstein Condensation and Superfluidity* (Oxford University Press, Oxford, 2016).
 [11] C. N. Yang, *Rev. Mod. Phys.* **34**, 694 (1962).
 [12] S. Stringari, *Sum Rules and Bose-Einstein Condensation*, in [77], p. 86.
 [13] A. J. Coleman and V. I. Yukalov, *Mod. Phys. Lett. B* **5**, 1679 (1991); *Nuovo Cimento* **107**, 535 (1992).
 [14] V. I. Yukalov, *Physica A* **310**, 413 (2002).
 [15] V. I. Yukalov, *Entropy* **22**, 565 (2020).
 [16] A. Colcelli, G. Mussardo, and A. Trombettoni, *Europhys. Lett.* **122**, 50006 (2018).
 [17] P. Nozières, *Some comments on Bose-Einstein Condensation*, in [77], p. 15.
 [18] G. D. Mahan, *Many-particles physics* (Plenum Press, New York, 1990), Chap. 10.
 [19] B. Capogrosso-Sansone, S. Giorgini, S. Pilati, L. Pollet, N. Prokof’ev, B. Svistunov, and M. Troyer, *New J. Phys.* **12**, 043010 (2010).
 [20] T. Giamarchi, *Quantum Physics in One Dimension* (Oxford University Press, Oxford, 2003).
 [21] M. A. Cazalilla, R. Citro, T. Giamarchi, E. Orignac, and M. Rigol, *Rev. Mod. Phys.* **83**, 1405 (2011).
 [22] E. H. Lieb and W. Liniger, *Phys. Rev.* **130**, 1605 (1963).
 [23] C. N. Yang and C. P. Yang, *J. Math. Phys.* **10**, 1115 (1969).
 [24] V. E. Korepin, N. M. Bogoliubov, and A. G. Izergin, *Quantum Inverse Scattering Method and Correlation Functions* (Cambridge University Press, Cambridge, 1993).
 [25] M. Gaudin, *The Bethe Wavefunction* (Cambridge University Press, Cambridge, 2014).
 [26] J.-S. Caux and P. Calabrese, *Phys. Rev. A* **74**, 031605(R) (2006).
 [27] M. Panfil and J.-S. Caux, *Phys. Rev. A* **89**, 033605 (2014).
 [28] J.-S. Caux, P. Calabrese, and N. A. Slavnov, *J. Stat. Mech.* (2007) P01008.
 [29] F. D. M. Haldane, *Phys. Rev. Lett.* **47**, 1840 (1981).
 [30] M. A. Cazalilla, *J. Phys. B: At. Mol. Opt. Phys.* **37**, S1 (2004).
 [31] T. Giamarchi, *AIP Conf. Proc.* **846**, 94 (2006).
 [32] G. Lang, *Correlations in Low-Dimensional Quantum Gases* (Springer, Cham, 2018).
 [33] G. Lang, F. Hekking, and A. Minguzzi, *SciPost Phys.* **3**, 003 (2017).
 [34] A. Shashi, M. Panfil, J.-S. Caux, and A. Imambekov, *Phys. Rev. B* **85**, 155136 (2012).
 [35] A. Lenard, *J. Math. Phys.* **5**, 930 (1964).
 [36] P. J. Forrester, N. E. Frankel, T. M. Garoni, and N. S. Witte, *Phys. Rev. A* **67**, 043607 (2003).
 [37] A. Colcelli, J. Viti, G. Mussardo, and A. Trombettoni, *Phys. Rev. A* **98**, 063633 (2018).
 [38] A. Colcelli, Ph.D. thesis, SISSA, 2020.
 [39] A. R. Its, A. G. Izergin, and V. E. Korepin, *Phys. Lett. A* **141**, 121 (1989); *Commun. Math. Phys.* **130**, 471 (1990); *Physica D* **53**, 187 (1991).
 [40] A. R. Its, A. G. Izergin, V. E. Korepin, and G. G. Varzugin, *Physica D* **54**, 351 (1992).
 [41] O. I. Patu and A. Klumper, *Phys. Rev. A* **88**, 033623 (2013).
 [42] V. L. Berezinskii, *Sov. Phys. JETP* **32**, 493 (1971).
 [43] J. M. Kosterlitz and D. J. Thouless, *J. Phys. C* **6**, 1181 (1973).
 [44] J. M. Kosterlitz, *J. Phys. C* **7**, 1046 (1974).
 [45] M. Le Bellac, *Quantum and Statistical Field Theory* (Oxford University Press, Oxford, 1991).
 [46] E. Simanek, *Inhomogeneous Superconductors* (Oxford University Press, Oxford, 1994).
 [47] H. Nishimori and G. Ortiz, *Elements of Phase Transitions and Critical Phenomena* (Oxford University Press, Oxford, 2010).
 [48] J. Villain, *J. Phys. (Paris)* **36**, 581 (1975).
 [49] H. Kleinert, *Gauge Fields in Condensed Matter—Vol. 1: Superflow and Vortex Lines* (World Scientific, Singapore, 1989).
 [50] G. Mussardo, *Statistical Field Theory: An Introduction to Exactly Solved Models in Statistical Physics* (Oxford University Press, Oxford, 2010).
 [51] D. R. Nelson and J. M. Kosterlitz, *Phys. Rev. Lett.* **39**, 1201 (1977).
 [52] N. V. Prokof’ev and B. V. Svistunov, *Phys. Rev. B* **61**, 11282 (2000).
 [53] M. Hasenbusch, *J. Phys. A* **38**, 5869 (2005).
 [54] W. Janke and K. Nather, *Phys. Rev. B* **48**, 7419 (1993).
 [55] R. Gupta, J. DeLapp, G. G. Batrouni, G. C. Fox, C. F. Baillie, and J. Apostolakis, *Phys. Rev. Lett.* **61**, 1996 (1988).
 [56] R. Gupta and C. F. Baillie, *Phys. Rev. B* **45**, 2883 (1992).
 [57] N. Schultka and E. Manousakis, *Phys. Rev. B* **49**, 12071 (1994).
 [58] Y. Komura and Y. Okabe, *J. Phys. Soc. Jpn* **81**, 113001 (2012).

- [59] N. Defenu, A. Trombettoni, I. Nándori, and T. Enss, *Phys. Rev. B* **96**, 174505 (2017).
- [60] I. Maccari, L. Benfatto, and C. Castellani, *Phys. Rev. B* **96**, 060508(R) (2017).
- [61] A. S. T. Pires, *Phys. Rev. B* **53**, 235 (1996).
- [62] M. Hasenbusch (private communication) (2019).
- [63] N. Prokof'ev, O. Ruebenacker, and B. Svistunov, *Phys. Rev. Lett.* **87**, 270402 (2001).
- [64] N. Prokof'ev and B. Svistunov, *Phys. Rev. A* **66**, 043608 (2002).
- [65] A. Trombettoni and A. Smerzi, and P. Sodano, *New J. Phys.* **7**, 57 (2005).
- [66] Z. Hadzibabic and J. Dalibard, *Riv. Nuovo Cimento* **34**, 389 (2011).
- [67] J. W. Kane and L. P. Kadanoff, *Phys. Rev.* **155**, 80 (1967).
- [68] V. N. Popov, *Theor. Math. Phys.* **11**, 565 (1972).
- [69] We observe that symmetrizing the density matrix adding the mirrored term in the region $L/2$ to L serves to have a positive and real result for the momentum distribution and occupation numbers, but it does not affect the scaling of the λ_k eigenvalues in terms of L .
- [70] N. Defenu, A. Codello, S. Ruffo, and A. Trombettoni, *J. Phys. A* **53**, 143001 (2020).
- [71] R. Seiringer, J. Yngvason, and V. A. Zagrebnoy, *J. Stat. Mech.* (2012) P11007.
- [72] M. Könenberg, T. Moser, R. Seiringer, and J. Yngvason, *New J. Phys.* **17**, 013022 (2015).
- [73] A. Khare, *Fractional Statistics and Quantum Theory* (World Scientific, Singapore, 2005).
- [74] F. Mancarella, A. Trombettoni, and G. Mussardo, *Nucl. Phys. B* **867**, 950 (2013); **887**, 216 (2014).
- [75] D. Lundholm and J. P. Solovej, *Commun. Math. Phys.* **322**, 883 (2013).
- [76] S. Ouvry and A. Polychronakos, *Nucl. Phys. B* **936**, 189 (2018); **949**, 114797 (2019).
- [77] *Bose-Einstein Condensation*, edited by A. Griffin, D. W. Snoke, and S. Stringari (Cambridge University Press, Cambridge, 1995).
- [78] P. A. Murthy, N. Defenu, L. Bayha, M. Holten, P. M. Preiss, T. Enss, and S. Jochim, *Science* **365**, 268 (2019).
- [79] T. Enss, *Phys. Rev. Lett.* **123**, 205301 (2019).
- [80] P. M. Preiss, J. H. Becher, R. Klemt, V. Klinkhamer, A. Bergschneider, N. Defenu, and S. Jochim, *Phys. Rev. Lett.* **122**, 143602 (2019).
- [81] D. Vodola, L. Lepori, E. Ercolessi, A. V. Gorshkov, and G. Pupillo, *Phys. Rev. Lett.* **113**, 156402 (2014).
- [82] M. Heyl, *Rep. Prog. Phys.* **81**, 054001 (2018).
- [83] D. T. Liu, J. Shabani, and A. Mitra, *Phys. Rev. B* **97**, 235114 (2018).
- [84] N. Defenu, T. Enss, and J. C. Halimeh, *Phys. Rev. B* **100**, 014434 (2019).
- [85] N. Defenu, G. Morigi, L. Dell'Anna, and T. Enss, *Phys. Rev. B* **100**, 184306 (2019).